Received: 22 September 2021 | Revised: 3 January 2022 | Accepted: 21 January 2022

DOI: 10.1002/hbm.25794

RESEARCH ARTICLE

WILEY

Characterizing multiscale modular structures in medication-free obsessive–compulsive disorder patients with no comorbidity

Xue Li[1,2] | Hailong Li[2,3] | Xi Jiang[1] | Jing Li[2] | Lingxiao Cao[2,3] | Jing Liu[2,3] | Haoyang Xing[1,2,3] | Xiaoqi Huang[2,3] | Qiyong Gong[2,3]

[1]College of Physics, Sichuan University, Chengdu, China

[2]Huaxi MR Research Center (HMRRC), Department of Radiology, West China Hospital of Sichuan University, Chengdu, China

[3]Research Unit of Psychoradiology, Chinese Academy of Medical Sciences, Chengdu, China

Correspondence
Haoyang Xing, College of Physics, Sichuan University, Chengdu 610041, China.
Email: xhy@scu.edu.cn

Xiaoqi Huang, Huaxi MR Research Center (HMRRC), Department of Radiology, West China Hospital of Sichuan University, Research Unit of Psychoradiology, Chinese Academy of Medical Sciences, Chengdu 610041, China.
Email: julianahuang@163.com

Funding information
National Natural Science Foundation of China, Grant/Award Number: 82027808; Key Research Project of Sichuan Science and Technology Department, Grant/Award Number: 2020YFS0048; Science Specialty Program of Sichuan University, Grant/Award Number: 2020SCUNL210

Abstract

Brain networks exhibit signatures of modular structure, which maintains a fine trade-off between wiring cost and efficiency of information transmission. Alterations in modular structure have been found in patients with obsessive–compulsive disorder (OCD). However, previous studies were focused on a single scale (i.e., modularity or intra/intermodular connectivity) for investigation. Here, we recruited 92 OCD patients and 90 healthy controls. A comprehensive analysis was performed on modular architecture alterations in the voxelwise functional connectome at the "global" (modularity), "meso" (modular segregation and within- and between-module connections), and "local" (participation coefficients, PC) scales. We also examined the correlation between modular structure metrics and clinical symptoms. The findings revealed that (1) there was no significant group difference in global modularity; (2) both primary modules (visual network, sensorimotor network) and high-order modules (dorsal attention network, frontoparietal network) exhibited lower modular segregation in OCD patients, which was mainly driven by increased numbers of between-module connections; and (3) OCD patients showed higher PC in several connectors including the bilateral middle occipital gyri, left medial orbital frontal gyrus, left superior frontal gyrus, left posterior cingulate gyrus, right superior temporal gyrus and right middle frontal gyrus, and lower PC in the right lingual gyrus. Moreover, these alterations in modular structure were associated with clinical symptoms in patients. Our findings provide further insights into the involvement of different modules in functional network dysfunction in OCD from a connectomic perspective and suggest a synergetic mechanism of module interactions that may be related to the pathophysiology of OCD.

KEYWORDS
graph theory, modularity, obsessive–compulsive disorder, resting-state fMRI

Xue Li and Hailong Li contributed equally to this study.

1 | INTRODUCTION

As a complex system, brain networks can be partitioned into modules, with connections that are highly interactive within modules but sparser between modules (Meunier, Achard, Morcom, & Bullmore, 2009; Newman & Girvan, 2004). Modular structure has been thought to promote greater resilience in the developmental process (Sporns & Betzel, 2016). Additionally, the modular structure of brain network organization maintains a fine trade-off between wiring cost and efficiency of information transmission (Bullmore & Sporns, 2012). Transdiagnostic dysfunctions in brain modules have been reported in patients with schizophrenia, bipolar disorder, and major depressive disorder (Ma et al., 2020).

Obsessive–compulsive disorder (OCD) is a neuropsychiatric disorder characterized by recurrent thoughts (obsessions) and/or repetitive behaviors (compulsions). Previous functional magnetic resonance imaging (fMRI) studies have found alterations in modular structure in OCD patients. At the global level, measures of modularity have yielded inconsistent results, with OCD patients showing lower modularity or nonsignificant differences compared to controls (Armstrong et al., 2016; Shin et al., 2014). At the network level, OCD patients showed elevated intramodular connectivity in the default mode network (DMN), central executive network (CEN) and salience network (SN) and altered intermodular connectivity between the SN and the DMN/CEN (Fan et al., 2017). Göttlich et al. found decreased intermodular connectivity between the limbic network and several other networks (i.e., the basal ganglia network, DMN, and frontoparietal network [FPN]) (Göttlich, Krämer, Kordon, Hohagen, & Zurowski, 2014). Increased connectivity was also found within the sensorimotor network (SMN), and decreased connectivity was found within the SN (Ye, Zhang, Fan, & Li, 2020). However, these studies investigated the altered modular structure of brain networks from only a single scale (i.e., modularity or intramodular and intermodular connectivity), which may result in information loss, and did not explore the effect of medication status in OCD patients.

In this study, we performed a comprehensive analysis on the modular architecture of the functional brain connectome on multiple scales in OCD patients. On the global scale, we calculated modularity to explore the overall modular properties of brain networks. On the mesoscale, we further calculated the modular segregation index and within- and between-module connections to identify module-specific characteristics. On the local scale, the alterations of nodes belonging to different modules were evaluated by participation coefficients. We also investigated the effects of medication use on the modular architecture of brain functional networks.

2 | METHODS

2.1 | Subjects

Ninety-three OCD patients diagnosed using the Structured Clinical Interview for DSM-IV Axis I Disorders (SCID) were recruited from the Mental Health Center, West China Hospital, Sichuan University. Among these patients, 79 patients were drug-naïve, and the remaining 14 patients had previously received medication (four clomipramine, three fluoxetine, three paroxetine, three sertraline, and one quetiapine). All the patients experienced a washout period for at least 4 weeks from any treatment before MRI scans. Ninety-two healthy control subjects (HCs) matched for sex and age were recruited via poster advertisements. The participants (aged 18–60) were all right-handed, and the exclusion criteria for both groups included (1) any history of major physical illness, cardiovascular disease or psychiatric or neurological disorder; (2) substance abuse or dependence; (3) inability to undergo an MRI scan; and (4) pregnancy. Additionally, OCD patients with a psychiatric comorbidity assessed using the SCID were excluded. The Yale-Brown Obsessive–Compulsive Scale (YBOCS) was used to evaluate OCD symptom severity, and anxiety and depressive symptoms were assessed using the 14-item Hamilton Anxiety Rating Scale (HAMA) and 17-item Hamilton Depression Rating Scale (HAMD), respectively. This study was approved by the Ethics Committee of the West China Hospital, Sichuan University. All subjects signed an informed consent form.

2.2 | Data acquisition and preprocessing

All fMRI data were acquired using a 3T GE Signa EXCITE MRI scanner with an 8-channel phase-array head coil. The following scanning parameters were used: number of slices = 30, repetition time (TR) = 2,000 ms, echo time (TE) = 30 ms, flip angle = 90°, slice thickness = 5 mm with no slice gap, field of view = 240 × 240 mm^2, and 200 volumes in each run. The T1-weighted spoiled gradient recall sequence was used with the following parameters: TR/TE = 8.5/3.4 ms, flip angle = 12°, slice thickness =1.0 mm, 156 contiguous coronal slices, and field of view = 240 ×240 mm^2. Image preprocessing was carried out using the Data Processing and Analysis of Brain Imaging (DPABI) toolbox (http://rfmri.org/dpabi). Preprocessing steps included discarding the first 10 volumes, slice timing correction, head-motion correction, spatial normalization to standard Montreal Neurological Institute space using the Diffeomorphic Anatomical Registration Through Exponentiated Lie algebra (DARTEL) algorithm, regression of nuisance covariates (cerebrospinal fluid signal, white matter signal, and Friston-24 motion parameters), linear detrending, smoothing with a 6-mm Gaussian kernel and bandpass filtering (0.01–0.08 Hz). To minimize the effects of head motion, we selected a stringent criterion; in particular, we excluded participants whose maximal head movement exceeded 2 mm in translation, whose mean frame displacement (FD) was more than 0.2 mm or whose rotation was more than 2°. One patient and two HCs were excluded due to excessive head motion.

2.3 | Functional network construction

We identified the seven cortical networks by mapping a widely used atlas (Yeo et al., 2011) onto the subject's brain in Montréal

Neurological Institute (MNI) standard brain atlas space. We chose Yeo's atlas because it is created from a whole-brain parcellation of 1,000 participants, and the atlas is very robust for investigating intrinsic brain networks, as they included multiple convergent methods to assess reliability (Yeo et al., 2011). Then, we extracted the time series of voxels within seven networks and calculated Pearson correlations between all pairwise voxels. A 39,080 × 39,080 connectivity matrix was constructed using Fisher's r-to-z transformation. The matrix was then thresholded over a sparsity of 1%, which preserved the strongest positive connections.

2.4 | Modular characteristics on the global scale and mesoscale

First, we calculated the modularity Q to characterize the global modular property of the functional network. Each voxel was labeled by functional systems (Yeo et al., 2011), and we adopted the measure of system segregation described in a previous study (Ma et al., 2020). For each module, the modular segregation index (MSI) was computed as follows:

$$\mathrm{MSI}_i = \frac{N_w - N_b}{N_w}, \quad (1)$$

where N_w is the number of connections within the same module, and N_b is the number of connections between a given module and other modules.

Then, we calculated the number of intramodular connections and intermodular connections to further explore which variable was responsible for driving the change in MSI.

2.5 | Modular characteristics on the local scale

Finally, we computed the participation coefficient to identify the extent to which a node was embedded in the module to which it belonged. The participation coefficient was defined as follows (Rubinov & Sporns, 2010):

$$P_i = 1 - \sum_m \left(\frac{D_i^m}{D_i}\right)^2, \quad (2)$$

where D_i^m is the connections of node i with voxels in module m (node i does not belong to module m), and D_i is the total number of connections with node i.

2.6 | Analysis of clinical correlations

Once statistically significant between-group differences were found, we explored the correlations between the abnormal metrics and clinical symptoms. Owing to the exploratory aim, we used a lenient statistical significance level of $p < .05$, uncorrected.

2.7 | Statistical analysis

A general linear model, including other covariables (age, sex and head motion), was adopted to estimate the effect of each modular characteristic. We used false discovery rate (FDR) correction for multiple comparisons, and the significance level was set at $p < .05$. All statistical analyses were performed using MATLAB.

2.8 | Effect of medication status and single sparsity bias

To investigate the potential effects of medication, we compared drug-naïve OCD patients with HCs and repeated the analysis. To avoid single sparsity bias (Du et al., 2015), we also used two other thresholds (2% and 0.5%) to validate the results. The details are described in Data S1, Supporting Information.

3 | RESULTS

3.1 | Demographic and clinical characteristics

We found no significant differences in sex or age between the patients and HCs. These results are summarized in Table 1.

3.2 | Modular characteristics on the global scale and mesoscale

All participants showed a strong modular architecture with Q values between 0.3 and 0.7 (Newman & Girvan, 2004). There was no significant group difference in global modularity.

We found significantly lower MSI values in the visual network (VIS) ($t = -3.735$, $p < .001$, FDR corrected), SMN ($t = -2.888$, $p = .008$, FDR corrected), dorsal attention network (DAN) ($t = -3.350$, $p = .002$, FDR corrected), and FPN ($t = -4.511$, $p < .001$, FDR corrected) in OCD patients compared with HCs (Figure 1a). Subsequent analyses found that these differences were mainly driven by a significantly decreased number of intramodular connections within the SMN ($t = -.3271$, $p = .009$, FDR corrected), along with increased numbers of intermodular connections between the VIS-DAN ($t = 3.247$, $p = .007$, FDR corrected), VIS-FPN ($t = 5.025$, $p < .001$, FDR corrected), VIS-DMN ($t = 2.931$, $p = .016$, FDR corrected), DAN-DMN ($t = 3.547$, $p = .003$, FDR corrected), FPN-ventral attention network (VAN) ($t = 2.854$, $p = .017$, FDR corrected) and VAN-DMN ($t = 4.600$, $p < .001$, FDR corrected) (Figure 1b).

TABLE 1 Demographic and clinical characteristics

Characteristics	OCD ($n = 92$)		HC ($n = 90$)		Analysis	
	Mean	*SD*	Mean	*SD*	t/χ^2	*p*-value
Sex (male/female)	57/35		55/35		0.01[a]	.91
Age (years)	29.42	13.00	28.34	10.85	0.74[b]	.46
Duration of illness (years)	7.39	5.53				
YBOCS score						
Obsessions	13.02	5.09				
Compulsion	8.38	5.33				
Total	21.40	5.51				
HAMA score	9.12	4.67				
HAMD score	9.03	5.24				

Abbreviations: HAMD, Hamilton Depression Scale; HAMA, Hamilton Anxiety Scale; HC, healthy control; OCD, obsessive–compulsive disorder; *SD*, standard deviation; YBOCS, Yale-Brown Obsessive–Compulsive Scale.

[a]Independent two-sample *t* test.

[b]Chi-square test.

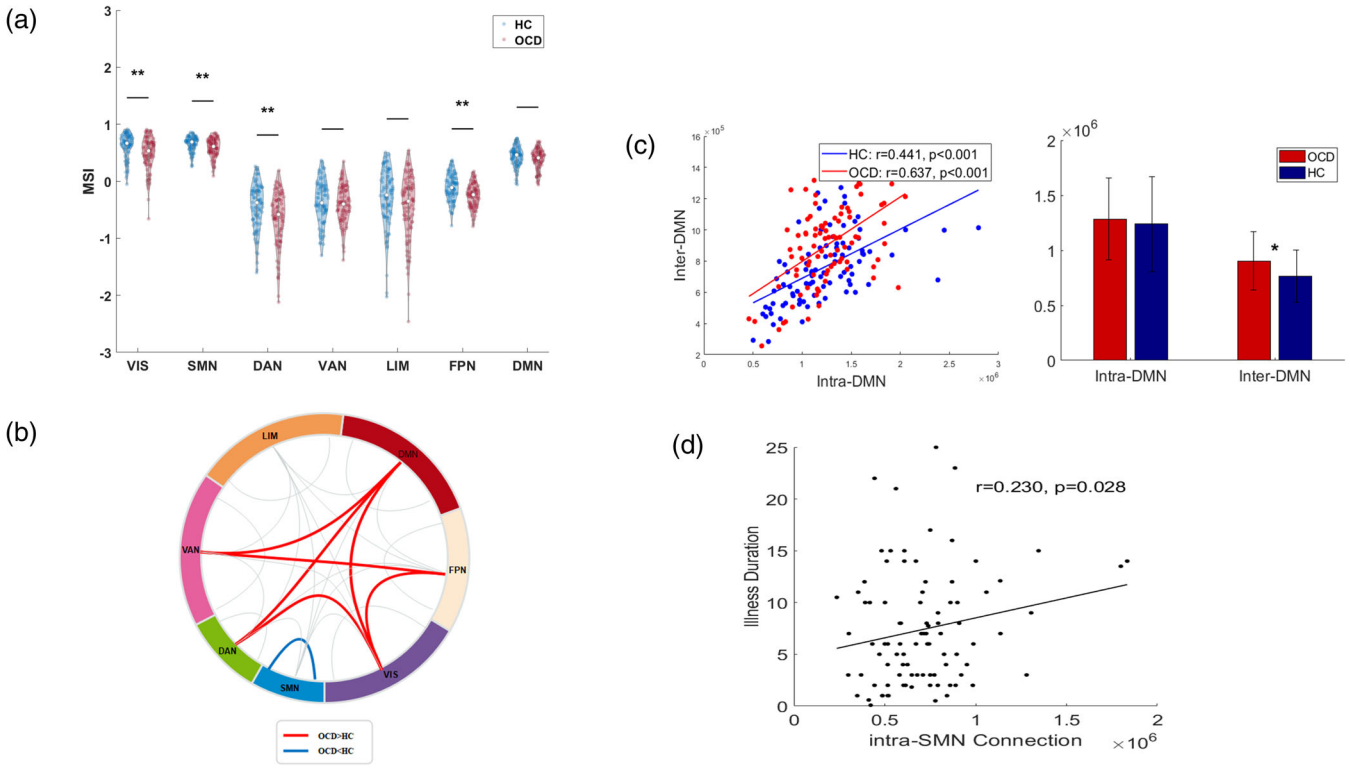

FIGURE 1 Group differences in module segregation index and intra/intermodular connections. (a) Differences in modular segregation index. (b) Differences in intramodular and intermodular connections. (c) Further analysis results in DMN on the mesoscale. (d) Correlations between clinical variables and modular structure in OCD patients. $^*p < .05$, $^{**}p < .01$, FDR corrected. DAN, dorsal attention network; DMN, default mode network; FDR, false discovery rate; FPN, frontoparietal network; HC, healthy control; LIM, limbic network; MSI, module segregation index; OCD, obsessive–compulsive disorder; SMN, sensorimotor network; VAN, ventral attention network; VIS, visual network

In particular, a significant group effect on MSI values was not found in the DMN, but we found that half of the statistical alterations in between-module connections were related to this network. This may be explained as the simultaneous increase of within and between module connections made the MSI in DMN showed no statistic difference. To support the suppose, we did further analyses. Based on the formula for MSI, the MSI in the DMN can be calculated as $MSI_{DMN} = 1 - \frac{N_b}{N_w}$. First, the correlation analysis between N_b (inter-DMN connection) and N_w (intra-DMN connection) indicated that inter-DMN connections were positively correlated with intra-DMN

connections (HC: $r = .637$, $p < .01$; OCD: $r = .441$, $p < .001$) in both HCs and OCD patients (Figure 1c), which suggests a similar trend that intra-DMN connections increased as the number of inter-DMN connections increased in both groups. Second, we separately compared the group differences in the inter-DMN connections and intra-DMN connections. We found that both inter- and intra DMN connections increased in OCD patients compared with HCs, but only inter-DMN connections reached significance ($p < .05$) (Figure 1c).

3.3 | Modular characteristics on the local scale

The significant between-group differences in PC are illustrated in Figure 2 and Table 2. The OCD patients had higher PC values in the bilateral middle occipital gyri (MOG) (left: $t = 6.735$, $p < .001$, FDR corrected; right: $t = 4.737$, $p = .002$, FDR corrected), left medial orbital frontal gyrus ($t = 4.647$, $p = .003$, FDR corrected), left superior frontal gyrus (SFG) ($t = 5.630$, $p < .001$, FDR corrected), left posterior cingulate gyrus ($t = 5.003$, $p = .002$, FDR corrected), right superior temporal gyrus ($t = 4.350$, $p = .006$, FDR corrected) and right middle frontal gyrus ($t = 5.100$, $p = .002$, FDR corrected), along with a significant lower value in the right lingual gyrus ($t = -5.216$, $p = .001$, FDR corrected).

3.4 | Correlation analysis and confounding effects

Regarding the correlation analysis, we observed positive correlations between the intramodular connections within the SMN and illness duration ($r = .230$, $p = .028$) (Figure 1d).

When controlling for the confounding causes of medication status and the sparsity values used, the results were largely consistent with the main findings (Data S1).

4 | DISCUSSION

In this study, we investigated the modular properties in patients with OCD from the global to the local scale. No significant difference was found on global scale. On the mesoscale, both primary modules (VIS and SMN) and high-order modules (DAN and FPN) exhibited lower MSI values in the OCD patients, which was mainly driven by an increased number of between-module connections. On the local scale, the topological role of several nodes showed abnormalities in the VIS and DMN modules. Additionally, medication status appeared to have no effect on our main findings. Taken together, the findings indicated a synergetic mechanism involving aberrant interactions among modules that may be related to cognitive deficits in OCD patients.

4.1 | Alterations of modular characteristics on the global scale and mesoscale

Compared with HCs, OCD patients exhibited no significant difference in global modularity, which was consistent with Shin's study (Shin et al., 2014) but contradicted another study (Armstrong et al., 2016) in which patients showed lower modularity. These discrepant findings may reflect the influence of OCD symptom dimensions and the effects of medication and comorbidities, which were well controlled in our study. In Shin's study, the OCD patients were drug-naïve or unmedicated for more than 4 weeks, which was consistent with our sample. While the Armstrong et al. performed graph-theoretical analysis in pediatric OCD, and some patients suffered from psychiatric comorbidities. Therefore, these discrepant findings may reflect the distinct alterations in global modularity in adult and pediatric OCD patients, and may also reflect the effect of comorbidities on the global modularity.

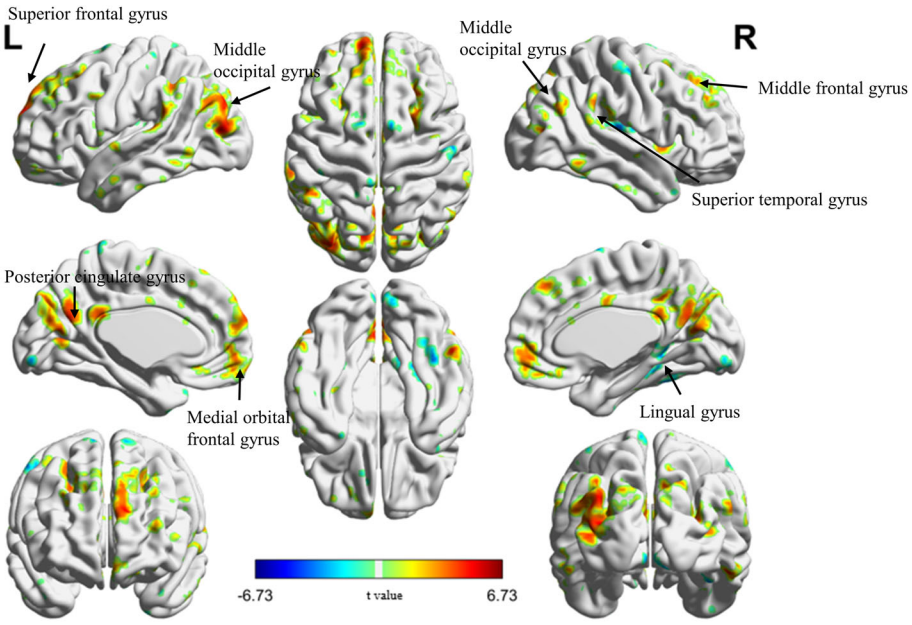

FIGURE 2 Differences in participation coefficients between OCD patients and HCs

TABLE 2 Group differences in participation coefficients

Contrast	Anatomical region of the peak voxel	Network	Cluster size (voxels)	MNI coordinates of peak voxel (*x*, *y*, *z*)	Peak *t* value
OCD > HC	Left middle occipital gyrus	VIS	860	−39, −81, 12	6.7347
	Left superior frontal gyrus	DMN	184	−12, 60, 24	5.6299
	Right middle frontal gyrus	FPN	159	30, 9, 54	5.1003
	Left medial orbital frontal gyrus	DMN	149	−9, 57, −6	4.6469
	Right superior temporal gyrus	VAN	82	66, −30, 21	4.3501
	Right middle occipital gyrus	VIS	75	33, −75, 18	4.7371
	Left posterior cingulate gyrus	DMN	65	−3, −39, 24	5.0029
OCD < HC	Right lingual gyrus	VIS	55	15, −45, 3	−5.2159

Note: Clusters showed significant differences between groups, $p < .05$, FDR corrected.
Abbreviations: DMN, default mode network; FDR, false discovery rate; FPN, frontoparietal network; HC, healthy control; MNI, Montreal Neurological Institute; OCD, obsessive–compulsive disorder; VAN, ventral attention network; VIS, visual network.

The modular architecture was characterized by a balance between the dense within-module connections and sparse between-module connections (Meunier et al., 2009). Intriguingly, we observed that the decreases in MSI values were mainly driven by the increased intermodular number of connections. We hypothesized that decreases in modular segregation may indicate a disrupted balance between module-specific specialization and integration in OCD.

We found module-level alterations in the primary modules VIS and SMN. Consistent with our results, reduced connectivity within visual and sensorimotor networks was previously found in OCD (Moreira et al., 2019). Intrusive imagery experienced by OCD patients was thought to be primarily visual (Coughtrey, Shafran, & Rachman, 2015). Previous studies have revealed impairments in visual processing in patients with obsessive–compulsive symptoms (Bhikram, Crawley, Arnold, Abi-Jaoude, & Sandor, 2020; Rampacher et al., 2010). The MSI changes in the VIS were driven by the increased number of intermodular connections, suggesting increased functional integration in OCD. Deviations in sensorimotor gating and sensorymotor integration have been reported in other OCD studies (Ahmari, Risbrough, Geyer, & Simpson, 2012; Russo et al., 2014), which supports the notion that the SMN may be involved in suppressing internally triggered intrusive and repetitive behaviors and thoughts. The decreased within-module connectivity within the SMN implied the enhancement of its functional specialization. In addition, correlation analyses found that intra-SMN connectivity positively correlated with illness duration, indicating that OCD patients bear increased or normalized intra-SMN connectivity with longer illness durations. Given the fact that there is a functional compensation of human brain (Fornito, Zalesky, & Breakspear, 2015), we hypothesized that there may be an adaptive process during the illness course of OCD, which increased intra-SMN connectivity with the extension of illness duration. Future longitudinal study will be needed to verify this hypothesis. This pattern of altered modular organization in primary modules may suggest that these networks play a crucial role in the pathophysiology of OCD, especially with the generation and inhibition of instructive thoughts.

High-order modules, such as the DAN and FPN, are thought to be involved in cognitive processing (Menon, 2011). Furthermore, the DAN is specialized for the top-down attention detection of behaviorally relevant stimuli (Vossel, Geng, & Fink, 2014), and the FPN plays a central role in cognitive control (Cole et al., 2013). Gürsel and colleagues found intra/internetwork dysconnectivity within and between the DMN, SN and FPN in OCD using a meta-analysis (Gürsel, Avram, Sorg, Brandl, & Koch, 2018). Our study excluded patients with psychiatric comorbidities, and all patients experienced a 4-week washout period, while the patients included in the meta-analysis did not. Meanwhile, the fMRI studies in this meta-analysis adopted a seed-based functional connectivity (FC) investigation method, and we performed graph analysis. Recently, Ferreira and colleagues have found hyperconnectivity in FPN during cognitive regulation, suggesting overactive cognitive regulation of external stimuli (Ferreira et al., 2021). Our results provide further evidence for the involvement of the DAN and FPN in cognitive modulation in OCD.

DMN plays an important role in the pathophysiology of OCD (Chen et al., 2019). Previous studies showed general dysconnectivity between the DMN and FPN, SN, and limbic network, as well as intra-DMN in OCD patients using resting-state functional connectivity analyses (Fan et al., 2017; Göttlich et al., 2014; Gürsel et al., 2018). In our study, we found that patients with OCD exhibited increased intermodular connectivity between DMN and VAN, DAN, and VIS, but no significant alterations in intra-DMN connection using graph-theoretical analyses. These discrepancies may be explained by the sample differences, such as the effect of medication and comorbidities, which were well controlled in our study. Besides, specific analytic methods adopted, like the selection of nodes and edges to construct the graph matrix and the diverse methods to identify networks may also influence the results.

4.2 | Alterations in participation coefficients on the local scale

The nodes that showed significant between-group differences in participation coefficients were mainly located in the VIS and DMN.

The MOG and lingual gyrus are located in the visual cortex region and may contribute to visual information processing of external

stimuli (de Gelder, Tamietto, Pegna, & van den Stock, 2015; Stern et al., 2017). A previous study demonstrated that category-selective attention modulated unconscious face/tool processing in the MOG in healthy adults (Tu, Qiu, Martens, & Zhang, 2013). Altered FC between the thalamus and MOG has been found in OCD patients, and FC was correlated with the severity of clinical symptoms (Chen et al., 2019; Li et al., 2019). Aberrant alterations in white matter and the surface area of the lingual gyrus have been found in OCD patients (Tao et al., 2017; Venkatasubramanian et al., 2012). Consequently, our results suggested that the increased PC of the MOG and lingual gyrus might provide support for disrupted visual information processing, which might cause some behavioral and cognitive symptoms of OCD.

The medial orbitofrontal cortex (mOFC), SFG, and left posterior cingulate cortex (PCC) are critical nodes in the DMN. There is a growing consensus that the DMN plays a key role in psychological processes in OCD (Cui et al., 2020; Gonçalves et al., 2017; Koch et al., 2018). The mOFC has been implicated in reward valuation (Du et al., 2020). Previous studies have provided evidence of molecular and functional abnormalities in the orbitofrontal cortex in OCD patients (Harrison et al., 2009; Piantadosi, Chamberlain, Glausier, Lewis, & Ahmari, 2021). The SFG is thought to be related to inhibitory control processes (Dippel, Mückschel, Ziemssen, & Beste, 2017), which were shown to be impaired in OCD patients (Chamberlain et al., 2007). One study suggested the role of the PCC in regulating attention in response to emotional stimuli (Ravindran et al., 2020). Abnormal FC in the PCC has been reported in OCD patients (Cui et al., 2020). Our findings contribute new evidence of the deep involvement, indicated by elevated PC values, of the nodes in the DMN that may explain the deficits related to inhibitory compulsive behaviors in OCD.

Several limitations of this study should be noted. First, our sample excluded patients with psychiatric comorbidities, and the conclusion may not be universal and cannot be generalized to all OCD patients. Second, although we found correlations between modular structure metrics and clinical symptoms, the results did not survive FDR corrections for multiple comparisons and should be validated in other samples. Third, subcortical networks, which are critically involved in prevailing neurobiological models of OCD, were not assessed in our study since the atlas we used does not include subcortical areas.

5 | CONCLUSIONS

In conclusion, we applied a comprehensive multiscale analysis of the modular structure of the functional connectome in OCD patients and HCs. Our findings provide further insights into the involvement of different modules in the functional network dysfunctions associated with OCD and suggest a synergetic mechanism of module interactions that may be related to the pathophysiology of OCD.

ACKNOWLEDGMENTS

This study was supported by the National Natural Science Foundation of China (Grant No. 82027808), the Key Research Project of Sichuan Science and Technology Department (Grant No. 2020YFS0048) and the Science Specialty Program of Sichuan University (Grant No. 2020SCUNL210).

CONFLICT OF INTEREST

The authors declare no potential conflict of interest.

ETHICS STATEMENT

This study was approved by the Ethics Committee of the West China Hospital, Sichuan University. All the enrolled participants provided fully informed written consent.

DATA AVAILABILITY STATEMENT

The data that support the findings of this study are available from the corresponding author upon reasonable request.

ORCID

Haoyang Xing https://orcid.org/0000-0002-9788-6412
Xiaoqi Huang https://orcid.org/0000-0001-8686-5010
Qiyong Gong https://orcid.org/0000-0002-5912-4871

REFERENCES

Ahmari, S. E., Risbrough, V. B., Geyer, M. A., & Simpson, H. B. (2012). Impaired sensorimotor gating in unmedicated adults with obsessive–compulsive disorder. *Neuropsychopharmacology*, *37*(5), 1216–1223. https://doi.org/10.1038/npp.2011.308

Armstrong, C. C., Moody, T. D., Feusner, J. D., McCracken, J. T., Chang, S., Levitt, J. G., … O'Neill, J. (2016). Graph-theoretical analysis of resting-state fMRI in pediatric obsessive–compulsive disorder. *Journal of Affective Disorders*, *193*, 175–184. https://doi.org/10.1016/j.jad.2015.12.071

Bhikram, T., Crawley, A., Arnold, P., Abi-Jaoude, E., & Sandor, P. (2020). Examining the functional activity of different obsessive–compulsive symptom dimensions in Tourette syndrome. *Neuroimage Clin*, *26*, 102198. https://doi.org/10.1016/j.nicl.2020.102198

Bullmore, E., & Sporns, O. (2012). The economy of brain network organization. *Nature Reviews. Neuroscience*, *13*(5), 336–349. https://doi.org/10.1038/nrn3214

Chamberlain, S. R., Fineberg, N. A., Menzies, L. A., Blackwell, A. D., Bullmore, E. T., Robbins, T. W., & Sahakian, B. J. (2007). Impaired cognitive flexibility and motor inhibition in unaffected first-degree relatives of patients with obsessive–compulsive disorder. *American Journal of Psychiatry*, *164*(2), 335–338. https://doi.org/10.1176/ajp.2007.164.2.335

Chen, Y., Meng, Z., Zhang, Z., Zhu, Y., Gao, R., Cao, X., … Fan, Q. (2019). The right thalamic glutamate level correlates with functional connectivity with right dorsal anterior cingulate cortex/middle occipital gyrus in unmedicated obsessive–compulsive disorder: A combined fMRI and (1)H-MRS study. *Australian and New Zealand Journal of Psychiatry*, *53*(3), 207–218. https://doi.org/10.1177/0004867418806370

Chen, Y., Ou, Y., Lv, D., Yang, R., Li, S., Jia, C., … Li, P. (2019). Altered network homogeneity of the default-mode network in drug-naive obsessive–compulsive disorder. *Progress in Neuro-Psychopharmacology & Biological Psychiatry*, *93*, 77–83. https://doi.org/10.1016/j.pnpbp.2019.03.008

Cole, M. W., Reynolds, J. R., Power, J. D., Repovs, G., Anticevic, A., & Braver, T. S. (2013). Multi-task connectivity reveals flexible hubs for adaptive task control. *Nature Neuroscience*, *16*(9), 1348–1355. https://doi.org/10.1038/nn.3470

Coughtrey, A. E., Shafran, R., & Rachman, S. J. (2015). Imagery in mental contamination. *Behavioural and Cognitive Psychotherapy*, *43*(3), 257–269. https://doi.org/10.1017/s1352465813000957

Cui, G., Ou, Y., Chen, Y., Lv, D., Jia, C., Zhong, Z., … Li, P. (2020). Altered global brain functional connectivity in drug-naive patients with obsessive–compulsive disorder. *Frontiers in Psychiatry*, *11*, 98. https://doi.org/10.3389/fpsyt.2020.00098

de Gelder, B., Tamietto, M., Pegna, A. J., & van den Stock, J. (2015). Visual imagery influences brain responses to visual stimulation in bilateral cortical blindness. *Cortex*, *72*, 15–26. https://doi.org/10.1016/j.cortex.2014.11.009

Dippel, G., Mückschel, M., Ziemssen, T., & Beste, C. (2017). Demands on response inhibition processes determine modulations of theta band activity in superior frontal areas and correlations with pupillometry—Implications for the norepinephrine system during inhibitory control. *NeuroImage*, *157*, 575–585. https://doi.org/10.1016/j.neuroimage.2017.06.037

Du, H. X., Liao, X. H., Lin, Q. X., Li, G. S., Chi, Y. Z., Liu, X., … Xia, M. R. (2015). Test-retest reliability of graph metrics in high-resolution functional connectomics: A resting-state functional MRI study. *CNS Neuroscience & Therapeutics*, *21*(10), 802–816. https://doi.org/10.1111/cns.12431

Du, J., Rolls, E. T., Cheng, W., Li, Y., Gong, W., Qiu, J., & Feng, J. (2020). Functional connectivity of the orbitofrontal cortex, anterior cingulate cortex, and inferior frontal gyrus in humans. *Cortex*, *123*, 185–199. https://doi.org/10.1016/j.cortex.2019.10.012

Fan, J., Zhong, M., Gan, J., Liu, W., Niu, C., Liao, H., … Zhu, X. (2017). Altered connectivity within and between the default mode, central executive, and salience networks in obsessive–compulsive disorder. *Journal of Affective Disorders*, *223*, 106–114. https://doi.org/10.1016/j.jad.2017.07.041

Ferreira, S., Moreira, P., Magalhães, R., Coelho, A., Marques, P., Portugal-Nunes, C., … Morgado, P. (2021). Frontoparietal hyperconnectivity during cognitive regulation in obsessive–compulsive disorder followed by reward valuation inflexibility. *Journal of Psychiatric Research*, *137*, 657–666. https://doi.org/10.1016/j.jpsychires.2020.11.008

Fornito, A., Zalesky, A., & Breakspear, M. (2015). The connectomics of brain disorders. *Nature Reviews. Neuroscience*, *16*(3), 159–172. https://doi.org/10.1038/nrn3901

Gonçalves, Ó. F., Soares, J. M., Carvalho, S., Leite, J., Ganho-Ávila, A., Fernandes-Gonçalves, A., … Sampaio, A. (2017). Patterns of default mode network deactivation in obsessive compulsive disorder. *Scientific Reports*, *7*, 44468. https://doi.org/10.1038/srep44468

Göttlich, M., Krämer, U. M., Kordon, A., Hohagen, F., & Zurowski, B. (2014). Decreased limbic and increased fronto-parietal connectivity in unmedicated patients with obsessive–compulsive disorder. *Human Brain Mapping*, *35*(11), 5617–5632. https://doi.org/10.1002/hbm.22574

Gürsel, D. A., Avram, M., Sorg, C., Brandl, F., & Koch, K. (2018). Frontoparietal areas link impairments of large-scale intrinsic brain networks with aberrant fronto-striatal interactions in OCD: A meta-analysis of resting-state functional connectivity. *Neuroscience and Biobehavioral Reviews*, *87*, 151–160. https://doi.org/10.1016/j.neubiorev.2018.01.016

Harrison, B. J., Soriano-Mas, C., Pujol, J., Ortiz, H., López-Solà, M., Hernández-Ribas, R., … Cardoner, N. (2009). Altered corticostriatal functional connectivity in obsessive–compulsive disorder. *Archives of General Psychiatry*, *66*(11), 1189–1200. https://doi.org/10.1001/archgenpsychiatry.2009.152

Koch, K., Reeß, T. J., Rus, O. G., Gürsel, D. A., Wagner, G., Berberich, G., & Zimmer, C. (2018). Increased default mode network connectivity in obsessive–compulsive disorder during reward processing. *Frontiers in Psychiatry*, *9*, 254. https://doi.org/10.3389/fpsyt.2018.00254

Li, K., Zhang, H., Yang, Y., Zhu, J., Wang, B., Shi, Y., … Zhang, H. (2019). Abnormal functional network of the thalamic subregions in adult patients with obsessive–compulsive disorder. *Behavioural Brain Research*, *371*, 111982. https://doi.org/10.1016/j.bbr.2019.111982

Ma, Q., Tang, Y., Wang, F., Liao, X., Jiang, X., Wei, S., … Xia, M. (2020). Transdiagnostic dysfunctions in brain modules across patients with schizophrenia, bipolar disorder, and major depressive disorder: A connectome-based study. *Schizophrenia Bulletin*, *46*(3), 699–712. https://doi.org/10.1093/schbul/sbz111

Menon, V. (2011). Large-scale brain networks and psychopathology: A unifying triple network model. *Trends in Cognitive Sciences*, *15*(10), 483–506. https://doi.org/10.1016/j.tics.2011.08.003

Meunier, D., Achard, S., Morcom, A., & Bullmore, E. (2009). Age-related changes in modular organization of human brain functional networks. *NeuroImage*, *44*(3), 715–723. https://doi.org/10.1016/j.neuroimage.2008.09.062

Moreira, P. S., Marques, P., Magalhães, R., Esteves, M., Sousa, N., Soares, J. M., & Morgado, P. (2019). The resting-brain of obsessive–compulsive disorder. *Psychiatry Research: Neuroimaging*, *290*, 38–41. https://doi.org/10.1016/j.pscychresns.2019.06.008

Newman, M. E., & Girvan, M. (2004). Finding and evaluating community structure in networks. *Physical Review. E, Statistical, Nonlinear, and Soft Matter Physics*, *69*, 026113. https://doi.org/10.1103/PhysRevE.69.026113

Piantadosi, S. C., Chamberlain, B. L., Glausier, J. R., Lewis, D. A., & Ahmari, S. E. (2021). Lower excitatory synaptic gene expression in orbitofrontal cortex and striatum in an initial study of subjects with obsessive compulsive disorder. *Molecular Psychiatry*, *26*(3), 986–998. https://doi.org/10.1038/s41380-019-0431-3

Rampacher, F., Lennertz, L., Vogeley, A., Schulze-Rauschenbach, S., Kathmann, N., Falkai, P., & Wagner, M. (2010). Evidence for specific cognitive deficits in visual information processing in patients with OCD compared to patients with unipolar depression. *Progress in Neuro-Psychopharmacology & Biological Psychiatry*, *34*(6), 984–991. https://doi.org/10.1016/j.pnpbp.2010.05.008

Ravindran, A., Richter, M., Jain, T., Ravindran, L., Rector, N., & Farb, N. (2020). Functional connectivity in obsessive–compulsive disorder and its subtypes. *Psychological Medicine*, *50*(7), 1173–1181. https://doi.org/10.1017/s0033291719001090

Rubinov, M., & Sporns, O. (2010). Complex network measures of brain connectivity: Uses and interpretations. *NeuroImage*, *52*(3), 1059–1069. https://doi.org/10.1016/j.neuroimage.2009.10.003

Russo, M., Naro, A., Mastroeni, C., Morgante, F., Terranova, C., Muscatello, M. R., … Quartarone, A. (2014). Obsessive–compulsive disorder: A "sensory-motor" problem? *International Journal of Psychophysiology*, *92*(2), 74–78. https://doi.org/10.1016/j.ijpsycho.2014.02.007

Shin, D. J., Jung, W. H., He, Y., Wang, J., Shim, G., Byun, M. S., … Kwon, J. S. (2014). The effects of pharmacological treatment on functional brain connectome in obsessive–compulsive disorder. *Biological Psychiatry*, *75*(8), 606–614. https://doi.org/10.1016/j.biopsych.2013.09.002

Sporns, O., & Betzel, R. F. (2016). Modular brain networks. *Annual Review of Psychology*, *67*, 613–640. https://doi.org/10.1146/annurev-psych-122414-033634

Stern, E. R., Muratore, A. F., Taylor, S. F., Abelson, J. L., Hof, P. R., & Goodman, W. K. (2017). Switching between internally and externally focused attention in obsessive–compulsive disorder: Abnormal visual cortex activation and connectivity. *Psychiatry Research: Neuroimaging*, *265*, 87–97. https://doi.org/10.1016/j.pscychresns.2016.08.006

Tao, J., Wang, X., Zhong, Z., Han, H., Liu, S., Wen, S., … Li, L. (2017). Alterations of white matter fractional anisotropy in unmedicated obsessive–compulsive disorder. *Neuropsychiatric Disease and Treatment*, *13*, 69–76. https://doi.org/10.2147/ndt.S123669

Tu, S., Qiu, J., Martens, U., & Zhang, Q. (2013). Category-selective attention modulates unconscious processes in the middle occipital gyrus. *Consciousness and Cognition*, *22*(2), 479–485. https://doi.org/10.1016/j.concog.2013.02.007

Venkatasubramanian, G., Zutshi, A., Jindal, S., Srikanth, S. G., Kovoor, J. M. E., Kumar, J. K., & Janardhan Reddy, Y. C. (2012). Comprehensive evaluation of cortical structure abnormalities in drug-naïve, adult patients with obsessive–compulsive disorder: A surface-based morphometry study. *Journal of Psychiatric Research*, *46*(9), 1161–1168. https://doi.org/10.1016/j.jpsychires.2012.06.003

Vossel, S., Geng, J. J., & Fink, G. R. (2014). Dorsal and ventral attention systems: Distinct neural circuits but collaborative roles. *Neuroscientist*, *20*(2), 150–159. https://doi.org/10.1177/1073858413494269

Ye, Q., Zhang, Z., Fan, Q., & Li, Y. (2020). Altered intramodular functional connectivity in drug naïve obsessive–compulsive disorder patients. *Annual International Conference of the IEEE Engineering in Medicine and Biology – Proceedings*, *2020*, 1734–1737. https://doi.org/10.1109/embc44109.2020.9175845

Yeo, B. T., Krienen, F. M., Sepulcre, J., Sabuncu, M. R., Lashkari, D., Hollinshead, M., … Buckner, R. L. (2011). The organization of the human cerebral cortex estimated by intrinsic functional connectivity. *Journal of Neurophysiology*, *106*(3), 1125–1165. https://doi.org/10.1152/jn.00338.2011

SUPPORTING INFORMATION

Additional supporting information may be found in the online version of the article at the publisher's website.

How to cite this article: Li, X., Li, H., Jiang, X., Li, J., Cao, L., Liu, J., Xing, H., Huang, X., & Gong, Q. (2022). Characterizing multiscale modular structures in medication-free obsessive–compulsive disorder patients with no comorbidity. *Human Brain Mapping*, *43*(7), 2391–2399. https://doi.org/10.1002/hbm.25794